STEM CELLS AND DEVELOPMENT
Volume 22, Number 1, 2013

DOI: 10.1089/scd.2012.0167

Ultraviolet B Preconditioning Enhances the Hair Growth-Promoting Effects of Adipose-Derived Stem Cells Via Generation of Reactive Oxygen Species

Yun-Mi Jeong,[1,2] Young Kwan Sung,[3] Wang-Kyun Kim,[1,2] Ji Hye Kim,[1,2] Mi Hee Kwack,[3] Insoo Yoon,[4] Dae-Duk Kim,[4] and Jong-Hyuk Sung[1,2]

Hypoxia induces the survival and regenerative potential of adipose-derived stem cells (ASCs), but there are tremendous needs to find alternative methods for ASC preconditioning. Therefore, this work investigated: (1) the ability of low-dose ultraviolet B (UVB) radiation to stimulate the survival, migration, and tube-forming activity of ASCs in vitro; (2) the ability of UVB preconditioning to enhance the hair growth-promoting capacity of ASCs in vivo; and (3) the mechanism of action for ASC stimulation by UVB. Although high-dose UVB decreased the proliferation of ASCs, low-dose (10 or 20 mJ/cm^2) treatment increased their survival, migration, and tube-forming activity. In addition, low-dose UVB upregulated the expression of ASC-derived growth factors, and a culture medium conditioned by UVB-irradiated ASCs increased the proliferation of dermal papilla and outer root sheet cells. Notably, injection of UVB-preconditioned ASCs into C_3H/HeN mice significantly induced the telogen-to-anagen transition and increased new hair weight in vivo. UVB treatment significantly increased the generation of reactive oxygen species (ROS) in cultured ASCs, and inhibition of ROS generation by diphenyleneiodonium chloride (DPI) significantly attenuated UVB-induced ASC stimulation. Furthermore, NADPH oxidase 4 (Nox4) expression was induced in ASCs by UVB irradiation, and Nox4 silencing by small interfering RNA, like DPI, significantly reduced UVB-induced ROS generation. These results suggest that the primary involvement of ROS generation in UVB-mediated ASC stimulation occurs via the Nox4 enzyme. This is the first indication that a low dose of UVB radiation and/or the control of ROS generation could potentially be incorporated into a novel ASC preconditioning method for hair regeneration.

Introduction

Adipose-derived stem cells (ASCs) show promise for tissue repair and regeneration, and can be easily isolated from subcutaneous fat collected via liposuction. These cells have demonstrated cytoprotective effects in various injury models. In particular, ASCs exert beneficial paracrine actions on surrounding cells through the secretion of multiple growth factors, including vascular endothelial growth factor (VEGF), hepatocyte growth factor (HGF), basic fibroblast growth factor (bFGF), keratinocyte growth factor (KGF), and platelet-derived growth factor [1–6]. Thus, the production and secretion of growth factors is an essential function of ASCs, and these growth factors in turn exert diverse pharmacological effects, such as angiogenesis, wound healing, and hair growth promotion [5,7–10]. External stimuli, such as hypoxia, induce the proliferation, migration, and paracrine activities of ASCs, leading to enhanced wound healing and hair growth promotion via the generation of reactive oxygen species (ROS) [7,8].

Ultraviolet B (UVB) light, like hypoxia, is an important mediator of ROS generation. UVB corresponds to electromagnetic radiation with a wavelength shorter compared with both visible light and UVA light and is in the range of 280–315 nm. UVB exposure induces the production of vitamin D in the skin, and the majority of health benefits attributed to short-term exposure to UVB radiation are related to this vitamin [11–13]. On the other hand, prolonged exposure to solar UV radiation may result in acute and chronic diseases, and overexposure to UVB can cause sunburn and some forms of skin cancer. Although Kim et al. showed that cytokines produced by keratinocytes and fibroblasts in

[1]Department of Applied Bioscience, CHA University, Seoul, Korea.
[2]Stem Cell Research Laboratory, CHA Stem Cell Institute, Seoul, Korea.
[3]Department of Immunology, School of Medicine, Kyungpook National University, Daegu, Korea.
[4]College of Pharmacy and Research Institute of Pharmaceutical Sciences, Seoul National University, Seoul, Korea.

response to UVB might be responsible for the reduction of adipogenesis in subcutaneous fat [14], the stimulatory effect of UVB light on ASCs isolated from this fatty tissue has not yet been demonstrated.

As noted above, culturing ASCs under hypoxic conditions results in their stimulation. However, there are practical requirements for the development of alternative ASC stimuli. Compared with the hypoxia chambers or incubators that are required for hypoxic preconditioning, UV irradiation is cost-efficient and relatively convenient to administer. Therefore, the current study queried (1) whether a low dose of UVB treatment as a novel preconditioning treatment would be sufficient to stimulate ASCs in vitro and enhance their hair growth-promoting effects in vivo, and (2) if so, what might be the potential mechanism of action involved. To address these important questions, we first compared the survival, migration, tube-forming activity, and paracrine actions of control and UVB-treated ASCs. The pivotal role of ROS generation by NADPH oxidase 4 (Nox4) was also investigated by pharmacologic and siRNA inhibition. Furthermore, the preconditioning effect of UVB in ASC-mediated hair regeneration was investigated in a C_3H/HeN mouse model.

Materials and Methods

Materials and antibodies

2′,7′-dichlorodihydrofluorescein diacetate (DCF-DA), 4′,6-diamidino-2-phenylindole (DAPI), diphenyleneiodonium chloride (DPI, a NADPH oxidase inhibitor), propidium iodide (PI), hydrogen peroxide (H_2O_2), and 3-(4, 5-dimethylthiazol-2-yl)-2, 5-diphenyltetrazolium bromide (MTT) were obtained from Sigma. Antibodies that recognize Akt, phospho-specific Akt (Ser473), extracellular signal-regulated kinase (ERK)1/2, phospho-specific ERK1/2, β-catenin, and phospho-specific β-catenin (ser675) were obtained from Cell Signaling. Anti-Nox4 and Ki-67 antibodies were obtained from Abcam. Antiactin antibody was purchased from Santa Cruz Biotechnology.

Cell cultures

ASCs were isolated from lipoaspirate of subcutaneous adipose tissue and characterized by flow cytometry using selected cell surface markers, as described previously [15]. ASCs were cultured in an alpha-Minimum Essential Medium (α-MEM) (Gibco/Invitrogen) with 10% fetal bovine serum (FBS; Gibco BRL). Human follicle dermal papilla (DP) cells were obtained from PromoCell and cultured in a Follicle Dermal Papilla Cell Growth Medium with a Supplement Mix (PromoCell) at 37°C in a 5% CO_2/95% air humidified atmosphere. Outer root sheath (ORS) cells were obtained and cultured as described previously [16] in an EpiLife Medium (Gibco/Invitrogen) with supplement mixtures plus penicillin–streptomycin in 5% CO_2 at 37°C.

UVB preconditioning

The UVB irradiation apparatus employed herein (BLE-1T158) was obtained from Spectronics Corp.. A Kodacel filter (TA401/407; Kodak) was used to eliminate light wavelengths of less than 290 nm (corresponding to ultraviolet C radiation). UV energy was measured using a Waldmann UV meter (model No. 585100; Waldmann Co., Villingen-Schwenningen, Germany). Before UVB irradiation, cells were washed with Dulbecco's phosphate-buffered saline (DPBS), and then incubated in fresh DPBS (0.5 mL/well). Then, cells were irradiated at the desired intensity within 5 min. After UVB irradiation, cells were returned to incubation in a basal medium (α-MEM/10% FBS), with treatments as described below at various time points before harvest.

Cell proliferation assay

Cells (5×10^3 cells/well) were seeded into 48-well plates. After UVB treatment in various doses, cells were incubated for 72 h at 37°C in 5% CO_2. Then, 50 μL/well of MTT solution (5 mg/mL) was added to measure metabolism and the plates were incubated for another 4 h. Supernatants were removed and formazan crystals were solubilized in dimethylsulfoxide. Viable cells were analyzed at 540 nm using an ELISA reader (Tecan).

In addition, proliferation of DP and ORS cells was measured after cells were incubated with a conditioned medium for 72 h.

Cell survival and apoptosis assays

ASCs were cultured on 6-well plates and treated with H_2O_2 (0.5 mM for 24 h) in the absence or presence of the UVB-preconditioning, as indicated. Plates were washed with phosphate-buffered saline (PBS) to remove dead floating cells, and the total number of surviving cells was determined by crystal violet staining to detect viable cells or PI staining to detect apoptotic cell nuclei. Images of the cells were captured using a fluorescence microscope (ECLIPSE E600; Nikon).

Migration assays

In the cell scratch migration assay, cells were grown in 6-well plates to 100% confluence and serum starved for 24 h. Perpendicular wounds were made by dragging a sterile plastic tip across the middle of each well, followed by washing with PBS. The widths of the wounds were measured in 10 randomly chosen fields. The migration rate (%) was expressed as the increase in migration relative to the untreated control.

Transwell migration assay was based on a modified Boyden Chamber assay [17]. The migration was monitored by observing the number of cells that moved through the filter. Migrated cells on the filters were quantified by the crystal violet assay. The transwell chambers were observed under phase-contrast microscopy with a Nikon microscope and an ocular grid at 0 and 24 h. Cells were photographed with a DCM300 digital camera (Scopetek).

Matrigel-based tube formation assay

Tube formation was evaluated using a modified Matrigel-based tube formation assay [18]. Each well of a 24-well plate was coated with Matrigel (Basement Membrane Matrix; BD Bioscience) according to the manufacturer's instructions and incubated at 37°C for 30 min. ASCs were detached from their original culture surfaces with 0.25% trypsin/ethylenediaminetetraacetic acid (EDTA), sedimented by centrifugation for

5 min, and resuspended in an endothelial growth medium (EGM2) cell culture medium. Cells were added to the Matrigel-coated wells and incubated at 37°C in 5% CO_2 for 16 h. Tube formation was observed using a phase-contrast microscope and photographed using a DCM300 digital camera. The tube length was evaluated using a GraphPad prism and presented as total tube length (mm) per high-power field.

Human angiogenesis array

Using the same condition of tube forming assay, protein samples were prepared using a cell lysis buffer of the Human Angiogenesis Array kit (R&D System). Expression of angiogenesis factors in ASCs was detected according to the manufacturer's guidance. Spot densities were quantified using a densitometer (Bio-Rad Laboratories). The background intensity was subtracted for analysis, and the data were normalized to the positive control.

Human growth factor antibody array

After 20 mJ/cm^2 UVB irradiation of ASCs in α-MEM, protein samples were prepared using the cell lysis buffer of Human Cytokine Antibody Array kit (RayBioTech). Growth factor expression was detected using a growth factor antibody array kit according to the manufacturer's guidance.

Reverse transcription–polymerase chain reaction

Total cellular RNA was extracted with TRIzol reagent (Gibco/Invitrogen) followed by reverse transcription (RT) using the cDNA synthesis kit (Promega). cDNA was synthesized from 1 μg total RNA using 200 U reverse transcriptase and 50 ng/μL oligo(dT). The cDNA obtained was amplified with the following primers: VEGF (5′-TACCTCCAC CATGCCAAGT-3′ and 5′-TGCATTCACA TTTGTTGTGC-3′), bFGF (5′-TGCTGGTGATGGGAGTT GTA-3′ and 5′-CCTCC AAGTAGCAGCCAAAG-3′), HGF (5′-CATGGACAAGATT GTTATCG-3′ and 5′-TCATTCAGC TTACTTGCATC-3′), and KGF (5′-TCTGTCGAACACAGTG GTACCT-3′ and 5′-GTG TGTCCATTTAGCTGATGCAT-3′), Nox4 (5′-CTTTTGGAAG TCCATTTGAG-3′ and 5′-GTCT GTTCTCTTGCCAAAAC-3′). Polymerase chain reactions (PCRs) were performed in a reaction mixture at a final volume of 25 μL. The reaction mixture contained 2 μL of the RT reaction mixture, 15 mM $MgCl_2$, 1.25 mM dNTP, 20 pM of each primer, and 0.5 U Taq polymerase (Promega).

Thermal cycling over 35 cycles consisted of an initial denaturation step at 94°C for 5 min, followed by denaturation at 94°C for 30 s, annealing at 56°C for 30 s, and extension at 72°C for 30 s. The reaction was terminated by final extension at 72°C for 5 min. The level of glyceraldehyde 3-phosphate dehydrogenase mRNA was used for sample standardization.

Western blot analysis

Protein samples were prepared in a RIPA buffer (50 mM Tris-HCl (pH 7.4), 150 mM NaCl, 1 mM EDTA, 1% Triton-X 100, 1% sodium dodecyl sulfate (SDS), 50 mM NaF, 1 mM Na_3VO_4, 5 mM dithiothreitol, 1 mg/mL leupeptin, and 1 mM phenylmethylsulfonyl fluoride). Samples were separated on 12%SDS-polyacrylamide gels and transferred to polyvinylidene fluoride membranes. The membranes were blocked with 5% dried milk in PBS containing 0.4% Tween-20, and then were incubated with the appropriate primary antibodies at a dilution of 1:1,000. Membrane-bound primary antibodies were detected with horseradish peroxidase (HRP)-conjugated secondary antibodies, and the Immobilon Western Chemiluminescent HRP Substrate flowed by exposure to Agfa X-ray film.

Preparation of conditioned medium

A conditioned medium derived from ASCs (ASC-CM) or UVB-preconditioned ASCs (UVB-CM) was prepared as described previously [19]. The conditioned medium was collected, centrifuged at 1,800 rpm for 10 min, and filtered through a 0.22-μm syringe filter. The filtrate was centrifuged in a 3-kDa molecular weight cutoff Vivaspin sample concentrator (Sartorius Stedim Biotech GmbH) and concentrated 2-fold (2×), 5-fold (5×), or 10-fold (10×).

Hair organ culture

Anagen hair follicles (HFs) were isolated from volunteer and cultured ex vivo, as described previously [16,20]. Briefly, dissected HFs were cut into small pieces (~2 mm in length from the bottom of the DP) and cultured in the Williams E medium (Gibco BRL) with 10 ng/mL hydrocortisone, 10 ng/mL insulin, 2 mM L-glutamine, and 100 U/mL penicillin at 37°C in 5% CO_2. ASC-CM (2×) or UVB-CM (2×) was added to the basal Williams E medium. After culturing for 3 or 6 days, HFs were harvested and stained with the anti-Ki-67 antibody and DAPI.

Patch assay

Mice were anesthetized in accordance with a protocol approved by the United States Pharmacopoeia and the Institutional Animal Care and Use Committee of Kyungpook National University.

Dorsal skin was harvested from C57BL/6 mouse neonates (P0) and incubated overnight with 100 mg/mL collagenase/dispase (Roche) at 4°C. The sample was subsequently digested with 0.25% trypsin in PBS at 37°C for 15 min, followed by filtration of the separated epidermal and dermal cells through 70- and 100-μm cell strainers, respectively (Becton Dickinson). Mouse neonatal dermal cells (10^6 cells) were incubated with ASC-CM or UVB-CM for 3 days, combined with cultured mouse neonatal epidermal cells in a ratio of 1:1, and resuspended in 100 μL of PBS (Supplementary Fig. S1; Supplementary Data are available online at www.liebertpub.com/scd). Cells were injected into the hypodermis of 7-week-old female Balb/c nude mice (Orient Bio). To verify HF induction, mice were sacrificed 2 weeks after cell implantation. HFs from 8 implantation sites from 4 different mice were counted by microscopic photography and morphometry.

ASC and ASC-CM injection into telogen-to anagen transition model

A dorsal area of 7-week-old C3H/HeN mice in the telogen stage of the hair cycle was shaved with a clipper and electric shaver, with special care taken to avoid damaging the bare skin [21]. Before they were injected into the mice, nonpreconditioned ASCs or UVB-preconditioned ASCs were

maintained at 37°C in 5% CO_2 for 4 h. Subcutaneous injections of non-preconditioned ASCs (1×10^4) or UVB-preconditioned ASCs (1×10^4), with or without DPI, were then injected into the dorsal skin of each mouse. Any darkening of the skin (indicative of hair growth) was carefully monitored. After 18 days, dorsal hair was shaved and its weight was measured.

In addition, 10-fold concentrated ASC-CM or UVB-CM were subcutaneously injected (50 μL) into the back of 7-week-old C3H/HeN mice, to measure the induction of telogen-to-anagen transition by UVB treatment. After 18 days, dorsal hair was shaved and its weight was measured.

ROS detection

ROS production in ASCs was measured using DCF-DA. After UVB irradiation, fluorescence images of the cells were taken with a fluorescence microscope (ECLIPSE E600; Nikon). In addition, fluorescence intensity of DCF-DA was measured and calculated using flow cytometry (Becon Dickinson) [7,8]. In the inhibition study, cells were pretreated with 100 nM DPI, and ROS generation was measured. To evaluate whether Nox4 might be involved in UVB-induced ROS generation in ASCs, human Nox4 siRNA and negative control siRNA were employed for ASC transfection [8]. ASCs were transfected with the siRNAs for 48 h with the use of lipofectamin^{TM}2000 (Gibco/Invitrogen). Immediately after UVB irradiation, cells were harvested using trypsin-EDTA and prepared for either flow cytometry using a flow cytometer from Becton Dickinson, or for fluorescence microcopy using an ECLIPSE E600 from Nikon.

Statistics

Differences among treatments were assessed by an analysis of variance, followed by the Dunnett's test. P values of <0.05 were taken to be significant.

Results

Effect of UVB irradiation on ASC proliferation

The effect of UVB irradiation on the proliferation of ASCs was first investigated in a dose range of 5–1,200 mJ/cm^2 (Fig. 1A). Low doses of UVB (5–50 mJ/cm^2) did not affect the proliferation of ASCs, whereas high doses (>100 mJ/cm^2) significantly decreased proliferation.

Effect of UVB on ASC survival

ASC viability was measured after H_2O_2 treatment (0.5 mM for 24 h) by crystal violet staining of living cells and PI staining of apoptotic nuclei. H_2O_2 treatment induced significant cell death, reflected by a decrease in the number of crystal violet-stained cells; however, a low dose of UVB

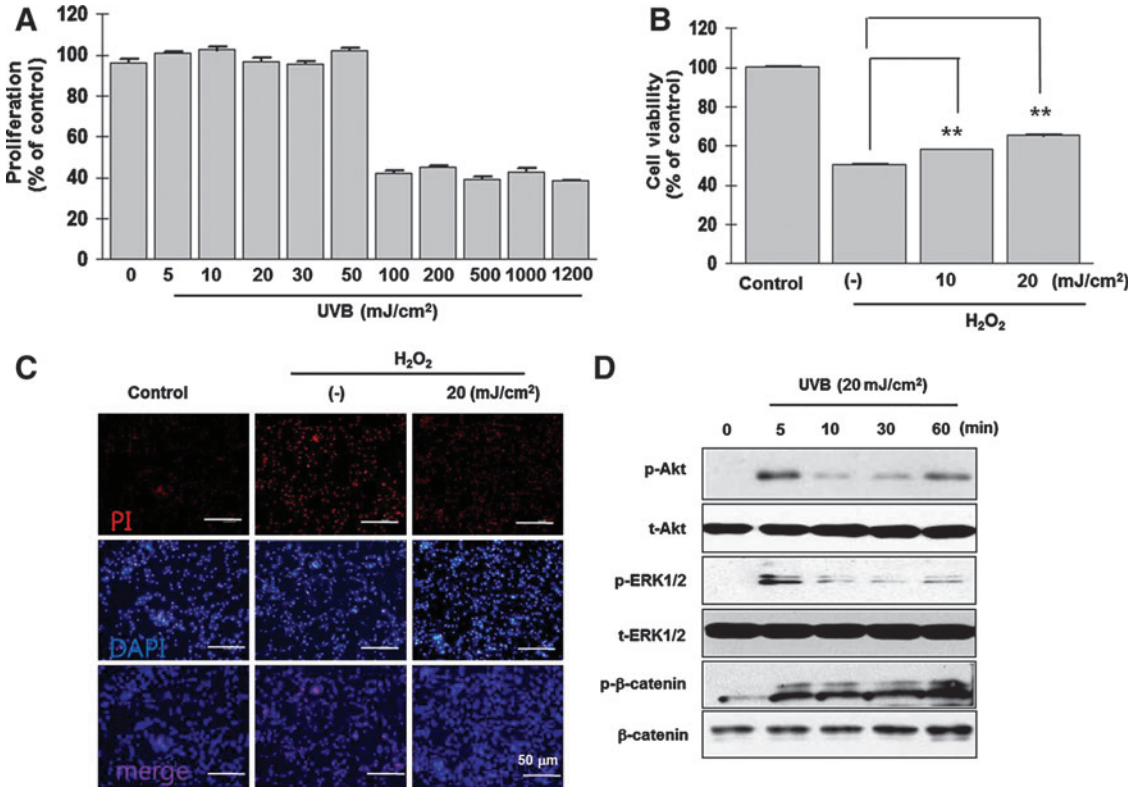

FIG. 1. Effect of UVB irradiation on the proliferation and survival of ASCs. **(A)** Proliferation was measured 72 h after UVB irradiation using MTT assay. A low-dose UVB exposure did not affect, while a high dose reduced the ASC proliferation. **(B)** H_2O_2 treatment (0.5 mM for 24 h) induced the cell death, but low-dose UVB preconditioning increased ASC survival. **(C)** H_2O_2 treatment enhanced the PI staining of ASC nuclei, which was attenuated by UVB irradiation. **(D)** Western blot analysis showed that the phosphorylation of survival-related signaling molecules was significantly increased by UVB treatment. $^{**}P<0.01$. UVB, ultraviolet B; ASCs, adipose-derived stem cells; H_2O_2, hydrogen peroxide; PI, propidium iodide. Color images available online at www.liebertpub.com/scd

irradiation (10 or 20 mJ/cm^2) before H_2O_2 treatment significantly increased the survival of ASCs (Fig. 1B, $P < 0.01$). Next, we tested whether UVB pretreatment could specifically reduce H_2O_2-induced apoptosis. Figure 1C shows that UVB irradiation (20 mJ/cm^2) decreased the number of PI-stained nuclei that resulted from H_2O_2 treatment. These data suggest that UVB preconditioning increased ASC survival by decreasing apoptosis.

Survival signal and expression of early undifferentiation marker

The phosphorylation of survival- or mitogen-related signaling molecules (i.e., Akt, β-catenin, and ERK1/2) was measured. UVB (20 mJ/cm^2) treatment significantly increased the phosphorylation of these signals within 5 min of exposure (Fig. 1D).

Although the mRNA expression levels of Nanog and the sex determining region Y-box 2 (Sox2) were not altered by exposure to UVB (data not shown), those of octamer-binding transcription factor 4 (Oct4), Rac exchanger 1 (Rex1), Krueppel-like factor 4 (klf4), and c-Myc were significantly increased by UVB irradiation at 4 h after UVB treatment (Supplementary Fig. S2).

Effect of UVB on ASC migration

Chamber (Fig. 2A) and cell scratch (Fig. 2B) migration assays were employed to assess the impact of UVB preconditioning on ASC migration. UVB irradiation (10 and 20 mJ/cm^2) significantly increased the migration of ASCs in a dose-dependent manner compared with untreated ASCs ($P < 0.01$).

UVB-induced tube formation

ASCs exhibit tube-forming activity on Matrigel in the EGM2 medium. Therefore, we examined whether UVB preconditioning could augment this ability. As shown in Fig. 2C, the tube-forming activity of ASCs was significantly increased by exposure to low-dose UVB ($P < 0.01$). In angiogenesis chip array, protein expression of coagulation factor III, urokinase-type plasminogen activator, HGF, and VEGF was induced in the EGM2 medium after 20 mJ/cm^2 UVB irradiation (Fig. 2D, $P < 0.01$).

Effect of UVB on secretion of paracrine factors

The regenerative ability of ASCs is primarily mediated by paracrine actions. Therefore, protein and mRNA expression levels of key growth factors were measured after UVB irradiation in α-MEM. First, growth factor expression was measured by the growth factor chip array. Compared with untreated cells, the spot density of 41 growth factors in UVB-treated ASCs was generally increased (data not shown). Among these elevated growth factors, we selected the most abundant proteins that differed between the UVB-irradiated and control cells, and that are reported to induce hair regeneration [22–28]. Based on these criteria, the protein expression levels of bFGF, KGF, HGF, and VEGF were found to be significantly increased by UVB preconditioning (Fig. 3A, $P < 0.01$).

In addition, mRNA expression of these growth factors was detected by RT-PCR. UVB treatment (10 and 20 mJ/cm^2) significantly upregulated the mRNA expression of bFGF, KGF, HGF, and VEGF in a dose-dependent manner at 4 h after UVB irradiation (Fig. 3B). Relative band densities were measured following pretreatment with UVB at a dose of 20 mJ/cm^2 and demonstrated significant differences between untreated and UVB-treated ASCs ($P < 0.01$).

Promotion of hair induction by UVB-CM treatment

The increased secretion of paracrine growth factors by UVB-irradiated ASCs could potentially lead to the enhancement of hair regeneration. To test this hypothesis, we evaluated the conditioned medium derived from UVB-treated ASCs

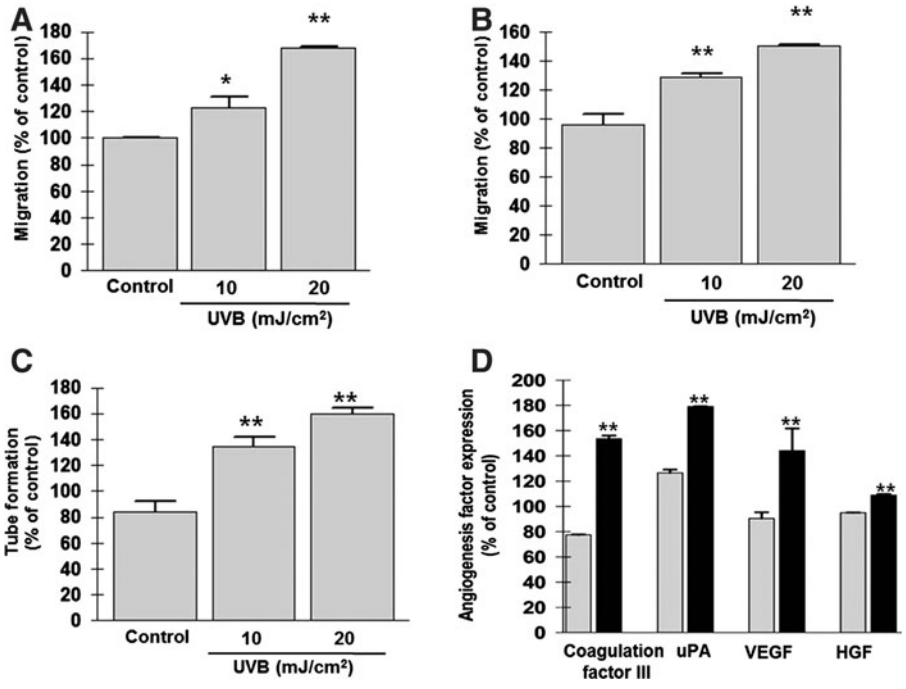

FIG. 2. Effect of UVB preconditioning on migration and tube-forming activities. **(A, B)** A low dose of UVB significantly increased the migration of ASCs in chamber **(A)** and cell scratch **(B)** migration assays. **(C)** Tube formation on Matrigel was enhanced by UVB irradiation, and tube length was measured. **(D)** In angiogenesis chip array, protein expression of coagulation factor III, uPA, VEGF, and HGF was upregulated in EGM2 after UVB radiation (*gray bars*: control, *black bars*: UVB treatment). $*P < 0.05$; $**P < 0.01$. uPA, urokinase-type plasminogen activator; VEGF, vascular endothelial growth factor; HGF, hepatocyte growth factor; EGM2, endothelial growth medium.

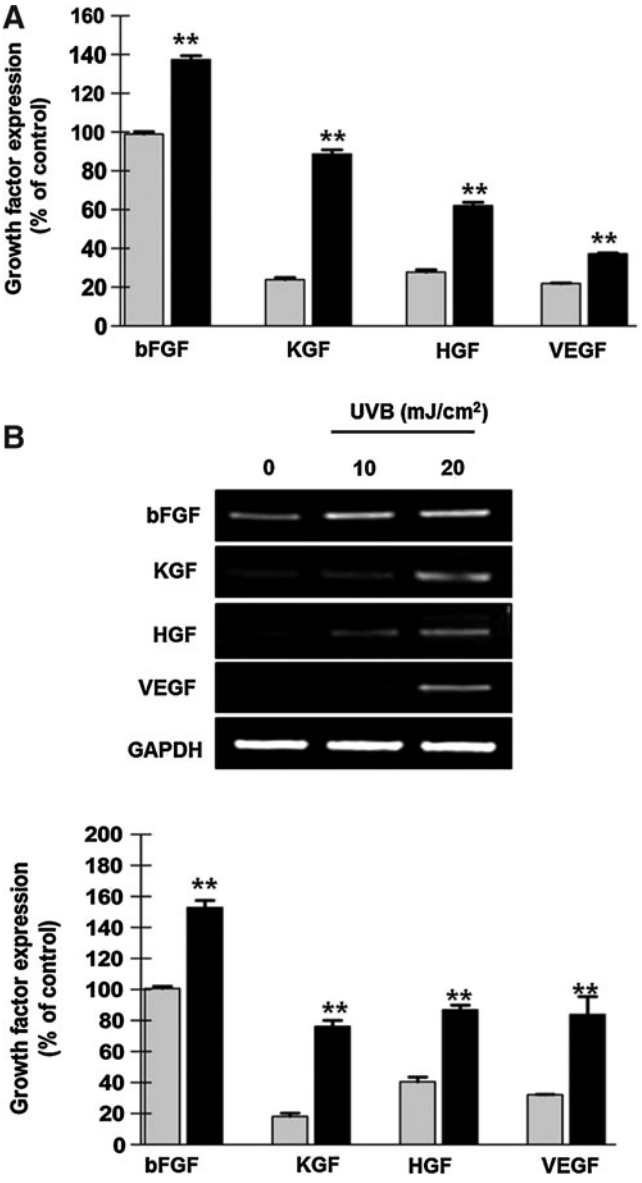

FIG. 3. Increased expression of growth factors following UVB preconditioning (*gray bars*; control, *black bars*: UVB treatment). **(A)** Growth factor chip array analysis showed that the protein expression of bFGF, KGF, HGF, and VEGF in ASCs was significantly induced by UVB treatment. **(B)** In addition, mRNA expression of these proteins was upregulated, as assessed by RT-PCR. Relative band densities revealed significant differences between control and UVB-treated cells. $^{**}P < 0.01$. bFGF, basic fibroblast growth factor; KGF, keratinocyte growth factor; RT-PCR, reverse transcription–polymerase chain reaction.

for the ability to stimulate new hair growth. HFs consist of various cells, including DP cells and ORS cells. We therefore explored whether UVB-CM versus ASC-CM could induce the proliferation of these cells. Compared with ASC-CM, UVB-CM (5- and 10-fold concentrated) significantly increased the proliferation of DP (Fig. 4A, $P < 0.01$) and ORS (Fig. 4B, $P < 0.01$) cells in vitro.

Because UVB-CM showed marked mitogenic effects on follicular DP and ORS cells, we investigated whether UVB-CM could also induce hair shaft elongation in isolated human anagen hairs. After the addition of ASC-CM or UVB-CM to the William's E medium, ex vivo hair organ culture was performed. After 6 days of organ culture, the length of HFs in the UVB-CM-enriched medium (2-fold concentrated) was significantly increased compared with ASC-CM (Fig. 4C, $P < 0.01$). In addition, anti-Ki-67 antibody (a marker of proliferating cells) staining of HFs showed that the number of Ki-67-positive matrix keratinocytes around the DP was significantly increased by UVB-CM treatment (Fig. 4D, $n = 7$ for each group, $P < 0.01$).

Using the patch assay (Supplementary Fig. S1), we next investigated whether UVB-CM could increase the hair induction potential of dermal cells in vivo. Compared with ASC-CM-treated dermal cells (control), transplantation of UVB-CM-treated dermal cells plus epidermal cells into nude mice induced ~16-fold greater number of HFs in nude mice (Fig. 4E, $n = 4$ for each group, $P < 0.01$).

Induction of telogen-to-anagen transition by UVB-treated ASCs

Compared with untreated control cells, subcutaneous injection of UVB-treated ASCs (ASC^{UVB}) significantly induced the telogen-to-anagen transition in C_3H/HeN mice at 14 days after ASC injection (Fig. 5A). Regenerated hair weight was measured at 18 days after injection and was found to be ~3-fold increased in the ASC^{UVB} group (Fig. 5B, $n = 5$ for each group, $P < 0.01$).

Induction of telogen-to-anagen transition by UVB-CM

Compared with ASC-CM, subcutaneous injection of UVB-CM (10-fold concentrated) significantly induced the telogen-to-anagen transition in C_3H/HeN mice at 14 days after ASC treatment (Fig. 5C). Regenerated hair weight was measured at 14 days and was found to be ~3.3-fold higher in the UVB-CM injection group (Fig. 5D, $n = 5$ for each group, $P < 0.01$).

ROS generation induced by UVB treatment

We next hypothesized that ROS generation in response to UVB treatment might be involved in the stimulation of ASCs and their subsequent ability to augment hair regeneration. Generation of ROS was examined using DCF-DA florescence dye, and indeed, UVB treatment visibly increased the fluorescence intensity of DCF-DA under fluorescence microscope observation (Fig. 6A). Inhibition of ROS generation by DPI treatment (at 100 nM concentration) reduced the signal intensity of DCF-DA. In addition, the fluorescence intensity of DCF-DA was alternatively measured using flow cytometry (Fig. 6B), and it was significantly increased by UVB treatment and attenuated by DPI treatment. Although DPI treatment did not have effect on UVB-untreated ASCs, DPI significantly attenuated the phosphorylation signaling molecules, such as Akt, β-catenin, and ERK1/2 in UVB-treated ASCs (data not shown). Furthermore, DPI treatment decreased the UVB-enhanced ASC migration (Fig. 6C), tube formation on Matrigel (Fig. 6D, $P < 0.01$), and mRNA expression of paracrine factors in ASCs (Fig. 6E). In our preliminary data, the telogen-to-anagen transition was measured and compared between a UVB-irradiated ASC

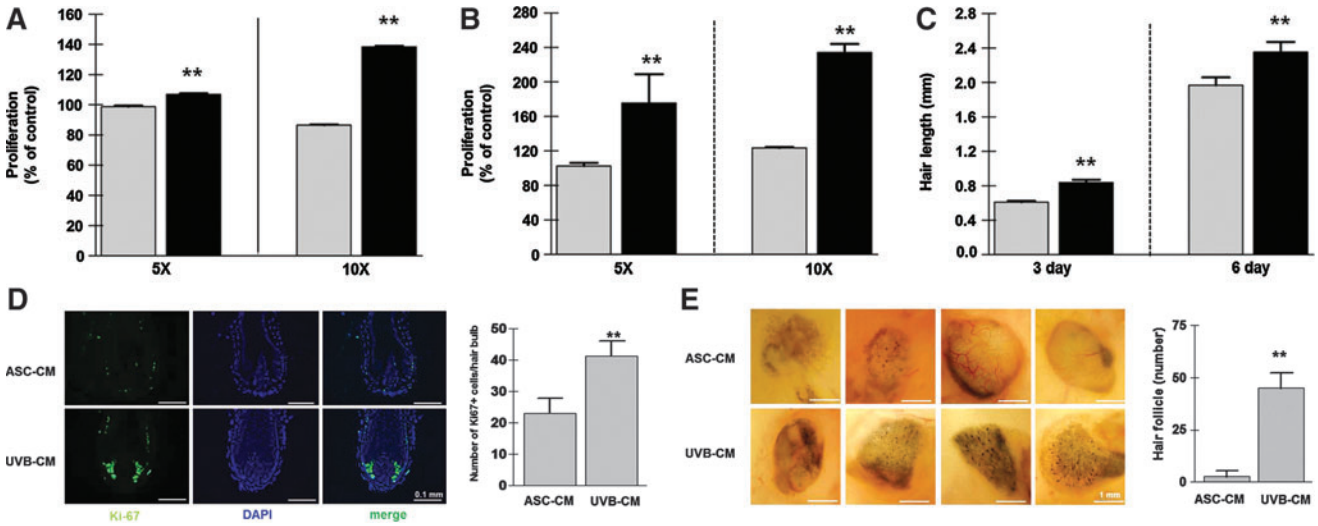

FIG. 4. Effect of UVB-CM on hair shaft elongation and hair induction. **(A, B)** Compared with ASC-CM (*gray bars*), UVB-CM (*black bars*) treatment significantly increased the proliferation of human dermal papilla cells **[(A)**, 5×; 5-fold concentrated CM, 10×; 10-fold concentrated CM], and outer root sheath cells **(B)**. **(C)** Hair shaft elongation was examined using isolated human anagen hairs. The length of HFs cultured in UVB-CM (*black bars*) was significantly elongated compared with ASC-CM (*gray bars*). **(D)** In addition, staining of HF with the Ki-67 antibody was significantly increased by UVB-CM treatment, and number of K67-positive cells was quantitated. **(E)** In the patch assay, transplantation of UVB-CM-treated dermal cells plus epidermal cells induced the new HFs. Number of HFs was significantly increased in the UVB-CM treated group. HFs were counted from 8 implantation sites from 4 different mice (2 sites/mouse, $n=4$ for each group). $^{**}P<0.01$. UVB-CM, UVB-preconditioned ASCs; ASC-CM, the conditioned medium derived from ASCs; HFs, hair follicles. Color images available online at www.liebertpub.com/scd

(ASC^{UVB}) injection and a DPI-pretreated and UVB-irradiated ASC ($ASC^{UVB+DPI}$) injection, which was also significantly decreased in the $ASC^{UVB+DPI}$-injected group (data not shown). Taken together, these results indicate that UVB-activated ASC stimulation and hair growth promotion are primarily mediated by Nox4-induced ROS generation.

Involvement of Nox4 in ROS generation

Because Nox4 is highly expressed and mediates ROS generation in ASCs [8], next confirmed whether UVB-induced ROS generation in ASCs is primarily mediated by Nox4 via specific Nox4 siRNA-silencing techniques. As shown in Fig. 7A, in Nox4-silenced ASCs, UVB treatment did not increase the ROS generation, again indicating that UVB-induced ROS levels are primarily generated by Nox4. Furthermore, UVB treatment did not increase the fluorescence intensity of DCF-DA in Nox4-silenced ASCs in flow cytometry (data not shown).

In addition, we tested whether intrinsic Nox4 expression could itself be induced by UVB treatment. A low dose of UVB significantly increased the mRNA (Fig. 7B) and protein (Fig. 7C) expression levels of Nox4 in ASCs, and both were reduced by DPI treatment (Fig. 7D, E). Although the

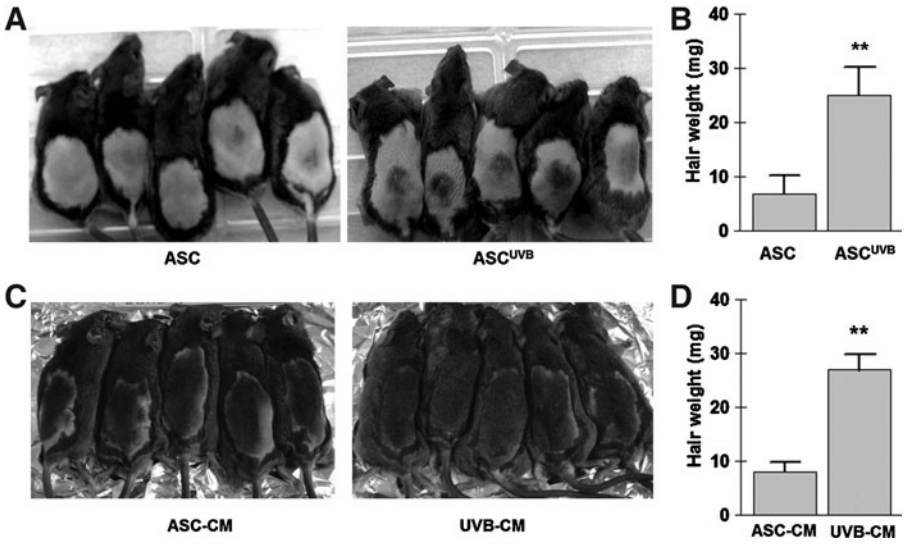

FIG. 5. Induced telogen-to-anagen transition by UVB preconditioning. After UVB irradiation, cells **(A, B)** or CM **(C, D)** were injected on the back of C3H/HeN mice. **(A)** Compared with untreated control ASCs, UVB treatment (ASC^{UVB}) significantly accelerated the telogen-to-anagen transition at 14 days. **(B)** In addition, hair weight was significantly increased in the ASC^{UVB} group at 18 days ($n=5$ for each group). **(C)** Compared with ASC-CM, subcutaneous injection of UVB-CM significantly induced the telogen-to-anagen transition at 14 days. **(D)** Hair weight was significantly increased in the UVB-CM injection group at 14 days ($n=5$ for each group). $^{**}P<0.01$.

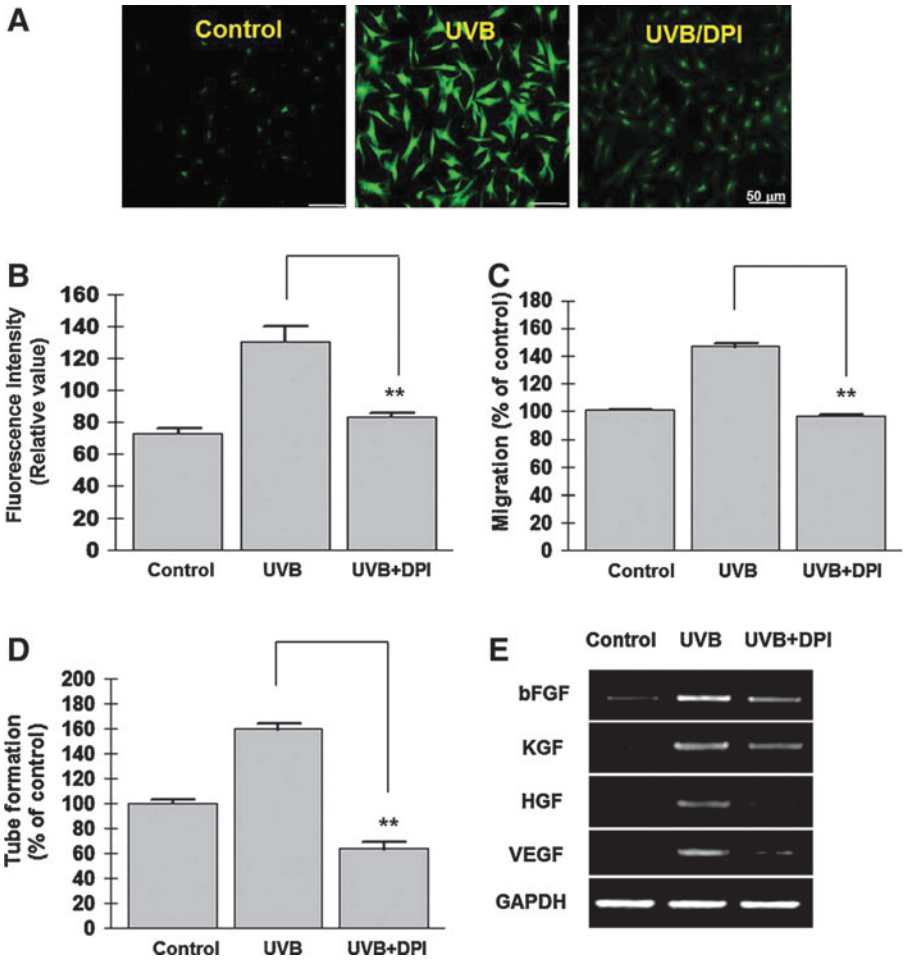

FIG. 6. ROS involvement in UVB-induced ASC stimulation. ROS generation was measured using DCF-DA by fluorescence microscopy **(A)** and flow cytometry **(B)**. **(A)** Fluorescence intensity of DCF-DA was visibly increased after 20 mJ/cm^2 UVB treatment, but pretreatment of DPI (100 nM) attenuated fluorescence signal of ASCs in microscopy. **(B)** ROS generation was alternatively measured by flow cytometry, and was also significantly reduced by DPI treatment. **(C, D)** DPI treatment (100 nM) attenuated the migration **(C)** and tube formation **(D)** of UVB-preconditioned ASCs. **(E)** DPI treatment also downregulated the mRNA expression of UVB-induced growth factors. $^{**}P < 0.01$. ROS, reactive oxygen species; DCF-DA, 2′,7′-dichlorodihydrofluorescein diacetate; DPI, diphenyleneiodonium chloride. Color images available online at www.liebertpub.com/scd

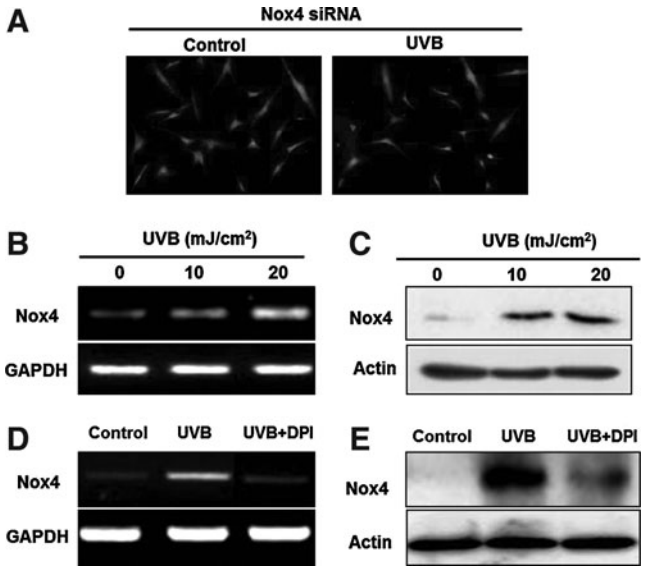

FIG. 7. Nox4 involvement in UVB-induced ROS generation. **(A)** UVB preconditioning did not induce the ROS generation in Nox4-silenced ASCs, as shown by DCF-DA fluorescence microscopy. **(B, C)** Nox4 mRNA and protein expression levels were both significantly increased by UVB treatment, demonstrated by RT-PCR **(B)** and western blot analysis **(C)**, respectively. **(D, E)** Inhibition of UVB-stimulated (20 mJ/cm^2) ROS generation by DPI treatment (100 μM). DPI significantly downregulated the mRNA **(D)** and protein **(E)** expression of Nox4.

mechanism for Nox4 induction by UVB has not been fully clarified, these results suggest that ROS generation might be involved in Nox4 upregulation indicative of a Nox4/ROS/Nox4 pathway.

Discussion

The primary goals of this work were to investigate whether UVB preconditioning could stimulate the functions of ASCs, including their hair growth-promoting effects. In addition, we aimed to elucidate the major mechanism of action of ASC stimulation by UVB irradiation. We found that a low dose of UVB (<20 mJ/cm^2) increased the survival, migration, angiogenic differentiation, and paracrine effects of ASCs in vitro. In addition, UVB preconditioning of ASCs before cell transplantation significantly increased hair weight and induced HF formation in mice. Furthermore, inhibition of ROS generation by DPI, a Nox inhibitor, attenuated the UVB-induced actions of ASCs. Finally, expression of the Nox4 enzyme itself was increased by UVB irradiation, and Nox4 silencing reduced ROS levels and UVB-induced functional enhancements in ASCs. Collectively, these results suggest that UVB preconditioning enhances the hair regenerative potential of ASCs via ROS generation and Nox4 upregulation.

To our knowledge, this is the first demonstration that UVB preconditioning can stimulate ASCs. However, other forms of preconditioning of stem cells before transplantation have

been applied to increase the regenerative potential of many different kinds of stem cells, including ASCs [3,29–32]. Hypoxia is the common method for preconditioning and has shown promising results in therapies for ischemic disease. For example, hypoxia increased the survival of ASCs, and the conditioned medium derived from hypoxia-preconditioned ASCs supported endothelial cell survival and endothelial tube formation [33]. Hypoxia preconditioning also enhanced the wound healing and hair-promoting capacities of ASCs [6,9,34]. However, hypoxia chambers and incubators are expensive pieces of equipment that are difficult to handle and maintain. For this reason, we sought to develop an alternative preconditioning method using low-dose UVB irradiation. The UVB-irradiation doses employed were lower than those usually used in photobiology studies. This is because UVB is a mutagen and high doses of UVB for activation may not meet with regulatory approval.

As noted above, UVB treatment, like hypoxia preconditioning, induced ASC survival, migration, angiogenesis, and growth factor secretion, all of which enhanced their hair growth-promoting functions. Although we did not directly compare the impact of UVB and hypoxia on the hair regenerative potential of ASCs, a low dose of UVB irradiation showed a similar efficacy as hypoxia for the stimulation of ROS generation and growth factor secretion. Therefore, it seems plausible that low-dose UVB could replace hypoxia as a means to precondition ASCs for the therapeutic treatment of various ischemic diseases.

Adipogenic differentiation of ASCs is regulated by various factors and the effect of ROS on adipogenic differentiation of ASCs is still controversial. Crop et al. discovered that inflammatory conditions affected the immunosuppressive capacity, morphology, and proliferation of ASCs, while their adipogenic differentiation capacity was unaffected [35]. In a preliminary study, we similarly investigated whether a low dose of UVB ($20\,mJ/cm^2$) could modulate the adipogenic differentiation of ASCs, but this was not the case (data not shown). However, hypoxic preconditioning (2% O_2) and the addition of low-dose chemical ROS donors significantly increased the adipogenic differentiation of ASCs in a previous study (data not shown). Although we did not further investigate the mechanism of action for the differences between hypoxic and UVB preconditioning, it is possible that long-term and mild exposure to ROS might induce the adipogenic differentiation of ASCs, while acute exposure to ROS might not.

Proliferative stem cells maintain a high ROS status and are extremely responsive to ROS donors [36–38]. In particular, ROS generation is mainly mediated by NADPH oxidase enzymes in stem/progenitor cells [39–41]. Among the Nox families, Nox4, Nox5, and dual oxidase 1 have all been detected in ASCs, but Nox4 is the most abundant of these [8]. Therefore, we investigated whether ROS generation by UVB irradiation is mediated by the Nox4 enzyme. In a functional study, Nox4 silencing by siRNA significantly reduced UVB-induced stimulation of ASCs. In addition, UVB treatment of ASCs significantly increased mRNA and protein expression of Nox4, and these increases were reversed by DPI. These results suggest that an intrinsic expression of Nox4 and an induced expression of Nox4 might actuate ROS generation during UVB preconditioning, collectively mediating the stimulation of ASCs.

Nitric oxide (NO) is a key signaling molecule in many types of stem cells, and NO synthase-NO-cGMP signaling is involved in the regulation of endothelial progenitor cells [42,43]. Therefore, we investigated whether UVB could generate NO and in this manner stimulate ASCs. However, treatment with *N*-nitro-L-arginine methyl ester [a NO synthase (NOS) inhibitor] failed to attenuate UVB-induced stimulation of ASCs (data not shown). Furthermore, mRNA expression levels of 3 types of NOS, inducible NOS, endothelial NOS, and neuronal NOS were barely detectable in ASCs (The expression levels were $\sim 2^8$-fold lower compared with Nox4 in unpublished data). In addition, treatment of ASCs with NO donors did not significantly induce the phosphorylation of mitogenic signals, such as Akt and ERK1/2. Thus, it is reasonable to assume that ROS generation by Nox4, but not NO, mediates the stimulation of ASCs after UVB irradiation.

Low-dose UVB irradiation significantly increased the survival, migration, paracrine effects, tube forming activity, and hair regenerative potential of ASCs. A mechanistic study showed that ROS generation via Nox4 mediates the stimulation of ASCs. This is the first indication that UVB treatment could be applied to a novel ASC priming method for hair regeneration. Furthermore, the induction of ROS levels in ASCs provides a novel strategy to precondition ASCs before cell transplantation.

Acknowledgments

This study was primarily supported by a grant from Basic Science Research Program through the National Research Foundation of Korea (2011-0019636).

Author Disclosure Statement

The authors declare no competing financial interests.

References

1. Wei X, Z Du, L Zhao, D Feng, G Wei, Y He, J Tan, WH Lee, H Hampel, et al. (2009). IFATS collection: the conditioned media of adipose stromal cells protect against hypoxia-ischemia-induced brain damage in neonatal rats. Stem Cells 27:478–488.
2. Kondo K, S Shintani, R Shibata, H Murakami, R Murakami, M Imaizumi, Y Kitagawa and T Murohara. (2009). Implantation of adipose-derived regenerative cells enhances ischemia-induced angiogenesis. Arterioscler Thromb Vasc Biol 29:61–66.
3. Rehman J, D Traktuev, J Li, S Merfeld-Clauss, CJ Temm-Grove, JE Bovenkerk, CL Pell, BH Johnstone, RV Considine and KL March. (2004). Secretion of angiogenic and anti-apoptotic factors by human adipose stromal cells. Circulation 109:1292–1298.
4. Song SY, HM Chung and JH Sung. (2010). The pivotal role of VEGF in adipose-derived-stem-cell-mediated regeneration. Expert Opin Biol Ther 10:1529–1537.
5. Chung HM, CH Won and JH Sung. (2009). Responses of adipose-derived stem cells during hypoxia: enhanced skin-regenerative potential. Expert Opin Biol Ther 9: 1499–1508.
6. Lee EY, Y Xia, WS Kim, MH Kim, TH Kim, KJ Kim, BS Park and JH Sung. (2009). Hypoxia-enhanced wound-healing function of adipose-derived stem cells: increase in stem cell

proliferation and up-regulation of VEGF and bFGF. Wound Repair Regen 17:540–547.
7. Kim JH, SH Park, SG Park, JS Choi, Y Xia and JH Sung. (2011).The pivotal role of reactive oxygen species generation in the hypoxia-induced stimulation of adipose-derived stem cells. Stem Cells Dev 20:1753–1761.
8. Kim JH, SY Song, SK Park, SU Song, Y Xia and JH Sung. (2012). Primary involvement of NADPH oxidase 4 in hypoxia-induced generation of reactive oxygen species in adipose-derived stem cells. Stem Cells Dev. [Epub ahead of print]; DOI:10.1089/scd.2011.0561.
9. Won CH, HG Yoo, OS Kwon, MY Sung, YJ Kang, JH Chung, BS Park, JH Sung, WS Kim and KH Kim. (2010). Hair growth promoting effects of adipose tissue-derived stem cells. J Dermatol Sci 57:134–137.
10. Lee MJ, J Kim, MY Kim, YS Bae, SH Ryu, TG Lee and JH Kim. (2010). Proteomic analysis of tumor necrosis factor-alpha-induced secretome of human adipose tissue-derived mesenchymal stem cells. J Proteome Res 9:1754–1762.
11. Grant WB. (2008). The effect of solar UVB doses and vitamin D production, skin cancer action spectra, and smoking in explaining links between skin cancers and solid tumours. Eur J Cancer 44:12–15.
12. Osmancevic A, K Landin-Wilhelmsen, O Larko, D Mellstrom, AM Wennberg, L Hulthen and AL Krogstad. (2007). UVB therapy increases 25(OH) vitamin D syntheses in postmenopausal women with psoriasis. Photodermatol Photoimmunol Photomed 23:172–178.
13. Prystowsky JH, PJ Muzio, S Sevran and TL Clemens. (1996). Effect of UVB phototherapy and oral calcitriol (1,25-dihydroxyvitamin D3) on vitamin D photosynthesis in patients with psoriasis. J Am Acad Dermatol 35:690–695.
14. Kim EJ, YK Kim, JE Kim, S Kim, MK Kim, CH Park and JH Chung. (2011). UV modulation of subcutaneous fat metabolism. J Invest Dermatol 131:1720–1726.
15. Kim WS, BS Park, JH Sung, JM Yang, SB Park, SJ Kwak and JS Park. (2007). Wound healing effect of adipose-derived stem cells: a critical role of secretory factors on human dermal fibroblasts. J Dermatol Sci 48:15–24.
16. Kwack MH, SH Shin, SR Kim, SU Im, IS Han, MK Kim, JC Kim and YK Sung. (2009). l-Ascorbic acid 2-phosphate promotes elongation of hair shafts via the secretion of insulin-like growth factor-1 from dermal papilla cells through phosphatidylinositol 3-kinase. Br J Dermatol 160:1157–1162.
17. Venge P. (1979). Kinetic studies of cell migration in a modified Boyden chamber: dependence on cell concentration and effects of the chymotrypsin-like cationic protein of human granulocytes. J Immunol 122:1180–1184.
18. Park SH, YM Jeong, JH Kim, HM Chung, W Suh, SH Sung, SG Park and JH Sung. (2011). Activation of vasculogenic progenitor cells by ent-16alpha,17-dihydroxy-kauran-19-oic acid. Biol Pharm Bull 34:1801–1807.
19. Kim WS, BS Park, HK Kim, JS Park, KJ Kim, JS Choi, SJ Chung, DD Kim and JH Sung. (2008). Evidence supporting antioxidant action of adipose-derived stem cells: protection of human dermal fibroblasts from oxidative stress. J Dermatol Sci 49:133–142.
20. Kwack MH, YK Sung, EJ Chung, SU Im, JS Ahn, MK Kim and JC Kim. (2008). Dihydrotestosterone-inducible dickkopf 1 from balding dermal papilla cells causes apoptosis in follicular keratinocytes. J Invest Dermatol 128:262–269.
21. Muller-Rover S, B Handjiski, C van der Veen, S Eichmuller, K Foitzik, IA McKay, KS Stenn and R Paus. (2001). A comprehensive guide for the accurate classification of murine hair follicles in distinct hair cycle stages. J Invest Dermatol 117:3–15.
22. Ozeki M and Y Tabata. (2002). Promoted growth of murine hair follicles through controlled release of vascular endothelial growth factor. Biomaterials 23:2367–2373.
23. Yano K, LF Brown and M Detmar. (2001). Control of hair growth and follicle size by VEGF-mediated angiogenesis. J Clin Invest 107:409–417.
24. Ozeki M and Y Tabata. (2002). Promoted growth of murine hair follicles through controlled release of basic fibroblast growth factor. Tissue Eng 8:359–366.
25. Jindo T, R Tsuboi, R Imai, K Takamori, JS Rubin and H Ogawa. (1994). Hepatocyte growth factor/scatter factor stimulates hair growth of mouse vibrissae in organ culture. J Invest Dermatol 103:306–309.
26. Jindo T, R Imai, R Tsuboi, K Takamori and H Ogawa. (1994). The effect of various cytokines on hair growth of mouse vibrissae in organ culture. J Dermatol Sci 7 Suppl 1:S73–S78.
27. Tomita Y, M Akiyama and H Shimizu. (2006). PDGF isoforms induce and maintain anagen phase of murine hair follicles. J Dermatol Sci 43:105–115.
28. Danilenko DM, BD Ring, D Yanagihara, W Benson, B Wiemann, CO Starnes and GF Pierce. (1995). Keratinocyte growth factor is an important endogenous mediator of hair follicle growth, development, and differentiation. Normalization of the nu/nu follicular differentiation defect and amelioration of chemotherapy-induced alopecia. Am J Pathol 147:145–154.
29. Sampat SR, GD O'Connell, JV Fong, E Alegre-Aguaron, GA Ateshian and CT Hung. (2011). Growth factor priming of synovium-derived stem cells for cartilage tissue engineering. Tissue Eng Part A 17:2259–2265.
30. Hwang NS, SG Im, PB Wu, DA Bichara, X Zhao, MA Randolph, R Langer and DG Anderson. (2011). Chondrogenic priming adipose-mesenchymal stem cells for cartilage tissue regeneration. Pharm Res 28:1395–1405.
31. Kim MS, CS Lee, J Hur, HJ Cho, SI Jun, TY Kim, SW Lee, JW Suh, KW Park, et al. (2009). Priming with angiopoietin-1 augments the vasculogenic potential of the peripheral blood stem cells mobilized with granulocyte colony-stimulating factor through a novel Tie2/Ets-1 pathway. Circulation 120:2240–2250.
32. Aly A, K Peterson, A Lerman, L Lerman and M Rodriguez-Porcel. (2011). Role of oxidative stress in hypoxia preconditioning of cells transplanted to the myocardium: a molecular imaging study. J Cardiovasc Surg (Torino) 52: 579–585.
33. Stubbs SL, ST Hsiao, HM Peshavariya, SY Lim, GJ Dusting and RJ Dilley. (2012). Hypoxic preconditioning enhances survival of human adipose-derived stem cells and conditions endothelial cells in vitro. Stem Cells Dev 21:1887–1896.
34. Park BS, WS Kim, JS Choi, HK Kim, JH Won, F Ohkubo and H Fukuoka. (2010). Hair growth stimulated by conditioned medium of adipose-derived stem cells is enhanced by hypoxia: evidence of increased growth factor secretion. Biomed Res 31:27–34.
35. Crop MJ, CC Baan, SS Korevaar, JN Ijzermans, M Pescatori, AP Stubbs, WF van Ijcken, MH Dahlke, E Eggenhofer, W Weimar and MJ Hoogduijn. (2010). Inflammatory conditions affect gene expression and function of human adipose tissue-derived mesenchymal stem cells. Clin Exp Immunol 162: 474–486.

36. Valle-Prieto A and PA Conget. (2010). Human mesenchymal stem cells efficiently manage oxidative stress. Stem Cells Dev 19:1885–1893.
37. Dernbach E, C Urbich, RP Brandes, WK Hofmann, AM Zeiher and S Dimmeler. (2004). Antioxidative stress-associated genes in circulating progenitor cells: evidence for enhanced resistance against oxidative stress. Blood 104: 3591–3597.
38. Le Belle JE, NM Orozco, AA Paucar, JP Saxe, J Mottahedeh, AD Pyle, H Wu and HI Kornblum. (2011). Proliferative neural stem cells have high endogenous ROS levels that regulate self-renewal and neurogenesis in a PI3K/Akt-dependant manner. Cell Stem Cell 8:59–71.
39. Ushio-Fukai M and N Urao. (2009). Novel role of NADPH oxidase in angiogenesis and stem/progenitor cell function. Antioxid Redox Signal 11:2517–2533.
40. Lange S, J Heger, G Euler, M Wartenberg, HM Piper and H Sauer. (2009). Platelet-derived growth factor BB stimulates vasculogenesis of embryonic stem cell-derived endothelial cells by calcium-mediated generation of reactive oxygen species. Cardiovasc Res 81:159–168.
41. Urao N, H Inomata, M Razvi, HW Kim, K Wary, R McKinney, T Fukai and M Ushio-Fukai. (2008). Role of nox2-based NADPH oxidase in bone marrow and progenitor cell function involved in neovascularization induced by hindlimb ischemia. Circ Res 103:212–220.
42. Sahara M, M Sata, T Morita, T Nakajima, Y Hirata and R Nagai. (2010). A phosphodiesterase-5 inhibitor vardenafil enhances angiogenesis through a protein kinase G-dependent hypoxia-inducible factor-1/vascular endothelial growth factor pathway. Arterioscler Thromb Vasc Biol 30:1315–1324.
43. Ii M, H Nishimura, A Iwakura, A Wecker, E Eaton, T Asahara and DW Losordo. (2005). Endothelial progenitor cells are rapidly recruited to myocardium and mediate protective effect of ischemic preconditioning via "imported" nitric oxide synthase activity. Circulation 111:1114–1120.

Address correspondence to:
Dr. Jong-Hyuk Sung
Department of Applied Bioscience
CHA University
#606-16, Yeoksam-dong, Kangnam-gu
Seoul 135-081
Korea

E-mail: brian99@empal.com

Received for publication March 30, 2012
Accepted after revision July 10, 2012
Prepublished on Liebert Instant Online July 11, 2012